

# Experimental Analysis of Viscoelastic Properties of Room Temperature Vulcanized Silicone based Magnetorheological Elastomer

Sandesh Bhaktha, Sriharsha Hegde\*, and Sathish Rao U.

*Manipal Institute of Technology, Manipal University, Manipal - 576 104, India*

*\*E-mail: sriharsha.hegde@manipal.edu*

## ABSTRACT

Magnetorheological Elastomers (MRE) endure a change in mechanical properties with the application of an externally applied magnetic field. It consists of an elastomeric matrix reinforced with ferromagnetic powdered particles. This paper focuses on the investigation of viscoelastic properties of Room Temperature Vulcanized (RTV) silicone based isotropic MRE in sandwich beam configuration by varying the volume percentage of Carbonyl Iron Powdered (CIP) reinforcement. Viscoelastic properties of the MRE core material were calculated by following the ASTM E756-05 standard. The magnetic field was applied by employing a Halbach array which was numerically analysed using Finite Element Method Magnetics (FEMM). The magnetic field was varied up to 0.15 T. Loss factor and shear modulus were found to be strongly influenced by the percentage content of CIP. The loss factor and shear modulus of 30% MRE at 0.15 T were higher than other tested samples. The variation of natural frequency with respect to the addition of CIP was validated numerically using Modal analysis conducted in Hyperworks.

**Keywords:** Magnetorheological elastomer; Halbach array; Finite element method magnetics; Free vibration test; Viscoelastic properties; Modal analysis

## NOMENCLATURE

$E$	Young's modulus of the base beam
$f_n$	Resonance frequency of base beam
$f_s$	Resonance frequency of sandwich beam
$G_1$	Shear modulus of the core material
$\eta_1$	Shear loss factor of the core material
$\eta_s$	Loss factor of sandwiched specimen
$\tau$	Shear stress of the core material
$\varphi$	Shear strain of the core material
$B$	Magnetic flux density

## 1. INTRODUCTION

Elastomers are one of the most used materials for vibration attenuation. Its viability to be successfully employed as a vibration damping material is dependent on its mechanical properties such as modulus and damping. In general, elastomers are flexible and possess high damping. But real-time operating conditions demand high load-bearing capacity along with good inherent damping characteristics. This problem is overcome by employing Magneto Rheological Elastomers (MRE), which undergo a change in rheological properties because of an externally applied magnetic field<sup>1-4</sup>. It comprises of a ferromagnetic ingredient embedded in a non-magnetic elastomeric material. The application of an external magnetic field causes the shear modulus and loss factor to change reversibly due to magnetic force between the particles. This behaviour depicted by them is termed as Magneto Rheological (MR) effect<sup>1,4-6</sup>.

MRE preparation is done by mixing a polymer-based matrix material with a ferromagnetic ingredient (reinforcement) during cross-linking. MRE cured in the magnetic field causes the ferromagnetic ingredients to orient themselves in the applied field direction imparting anisotropic properties to it. In isotropic MRE, the ferromagnetic particles are arbitrarily arranged inside the matrix. Anisotropic MRE shows better MR effect compared to isotropic MRE<sup>4,7</sup>. MR effect exhibited by these materials mainly depends upon the magnitude of the magnetic flux density<sup>8,9</sup>, size<sup>10</sup> and shape<sup>11</sup> of the Ferromagnetic particles, its volume percentage<sup>5,6,10,12</sup>, type of the elastomeric matrix employed<sup>8</sup> and orientation of iron particles in the matrix<sup>4,7</sup>. Silicone elastomer is the most suitable matrix material for the MRE since it can be easily processed, are easy to handle, and possess a wide range of working temperatures<sup>4</sup>. Carbonyl Iron Powder (CIP) is used as reinforcement due to high permeability, high magnetic saturation, and very low or zero remanent magnetisation. These unique characteristics make MRE a viable material in Noise, Vibration, and Harshness (NVH) related applications<sup>13-15</sup> as well as Vibration control systems<sup>2,16</sup>.

Viscoelastic properties of elastomers are usually characterised by carrying out experiments employing dynamic mechanical analyser (DMA)<sup>17</sup> and Rheometer<sup>18</sup>. Parallel plate Rheometers in oscillatory, squeeze, and stress-controlled mode are employed by many researchers to evaluate the rheological properties of MRE. The damping properties of MR elastomers are also characterised using DMA. The current work focuses on characterizing MR elastomers by employing a relatively economical way by making use of the ASTM standard. The

investigation of viscoelastic properties of Silicone-based isotropic MRE with respect to percentage content of CIP and the magnetic field is carried out using ASTM- E756-05<sup>19</sup>. Viscoelastic property characterisation of MRE using the ASTM method has not been reported in literature so far. Also, in the current work, a relatively inexpensive way of experimentally determining the damping characteristics and shear properties of MRE has been employed instead of bulky and expensive methods like Rheometer and DMA. The combined effect of iron powder and magnetic field on the natural frequency of the fabricated MRE sandwich beam has been experimentally studied. The magnetic field effects are investigated by using the Halbach array to apply the magnetic field to the MRE cantilever beam.

## 2. THEORETICAL BACKGROUND

In the current study, the methodology was adopted as per ASTM E-756-05 (cantilever beam configuration)<sup>19</sup> for determining the viscoelastic properties of the core material. For any viscoelastic material, the loss factor ( $\eta_1$ ) and shear modulus ( $G_1$ ) according to the ASTM standard is given by

$$\eta_1 = \frac{(A\eta_s)}{\left[ A - B - 2(A - B)^2 - 2(A\eta_s)^2 \right]} \quad (1)$$

$$G_1 = \left[ A - B - 2(A - B)^2 - 2(A\eta_s)^2 \right] \times \left[ \frac{(2\pi C_1 E H H_1)}{l^2 \left\langle (1 - 2A + 2B)^2 + 4(A\eta_s)^2 \right\rangle} \right] \quad (2)$$

where

$$A = \left( \frac{f_s}{f_n} \right)^2 (2 + DT) \left( \frac{B}{2} \right) \quad (3)$$

$$B = \frac{1}{\left[ 6(1 + T)^2 \right]} \quad (4)$$

$\eta_s$  = loss factor of the sandwich specimen and  $f_s$  = natural frequency for mode  $n$  of the sandwich specimen is determined experimentally by conducting the free vibration test.  $f_n$  = natural frequency for  $n^{\text{th}}$  mode of base beam.  $H$  and  $H_1$  are thickness of base beam and core material.  $\rho$  and  $\rho_1$  are the densities of the base beam and core material.  $D$  is the density ratio ( $\rho_1/\rho$ ) and  $T$  is the thickness ratio ( $H/H_1$ ).  $E$  is the Young's modulus of the base beam.  $C_1 = 0.5595$  (coefficient for mode 1).

The amplitude of the successive peaks is noted from the free vibration response graph and the damping ratio ( $\zeta$ ) of the sandwich specimen is calculated using the Eqn (5).

$$\ln \frac{x_0}{x_1} = \frac{2\pi\zeta}{\sqrt{1 - \zeta^2}} \quad (5)$$

where

$x_0, x_1$  – successive response from the free vibration response graph

$\zeta$  – Damping ratio of the sandwich specimen

The loss factor ( $\eta_s$ ) of the sandwich specimen is calculated using the equation,

$$\eta_s = 2\zeta \quad (6)$$

## 3. METHODOLOGY

### 3.1 Fabrication of MRE Sandwich beam

The dimensions of the sandwich beam specimens were determined from ASTM standard E 756-05. It consists of a core (thickness 6mm) sandwiched between two Aluminium beams (1.7mm thickness). The MRE core is prepared by mixing the matrix (Silastic 3483 base from Dow Corning Corporation) with Carbonyl iron particles 5  $\mu\text{m}$  in diameter (Chengdu Nuclear, China) and adding a curing agent (Silastic 83). The sample is then subjected to degasification. The prepared mixture is gushed into an acrylic mould of dimensions 180mm x 10mm x 6mm, which is followed by curing at room temperature without applying any magnetic field for 24 hours. This renders isotropic nature to the prepared samples. 7 samples with varying percentage content of CIP (shown in Table 1) were prepared. The Aluminium base beams of same dimensions and natural frequencies ( $f_n$ ) are bonded to the MRE core using a synthetic rubber based adhesive and is cured for 24 hours. In the root section (used to facilitate the clamping of specimen in the test fixture), an Aluminium spacer of length 25mm and thickness same as the core material is glued to the base beams using cyanoacrylate adhesive.

**Table 1. Percentage by volume content of CIP of samples**

Sample number	Percentage content of CIP
1	0
2	5
3	10
4	15
5	20
6	25
7	30

### 3.2 Halbach Array to Apply Magnetic Field

To produce magnetic field, Neodymium rare earth permanent magnets are placed (Fig. 1(a)) following the Halbach's arrangement<sup>20</sup>. The magnetic flux density thus produced using the arrangement of magnets was predicted by performing a simulation using finite element method magnetics (FEMM)<sup>21</sup>. The results of the simulation and the plot of field variation between the poles are shown in Fig. 1(b) and Fig. 1(c). Based on the results obtained from simulation, permanent magnets were arranged. Measurement of the magnetic flux density was quantified using a Gauss meter.

### 3.3 Experimental Setup for Conducting Free Vibration Test

Free vibration test is conducted on the sandwich specimen to determine its natural frequency ( $f_s$ ) and loss factor ( $\eta_s$ ). The setup used to conduct the experiment is depicted in Fig. 2. The magnitude of the magnetic flux density is adjusted by varying the air gap distance between the permanent magnets using a screw-nut arrangement. An accelerometer (PCB piezotronics, Sensitivity – 100.6 mV/g) is positioned at the unclamped beam end. The acceleration signals are acquired using NI – 9234 data

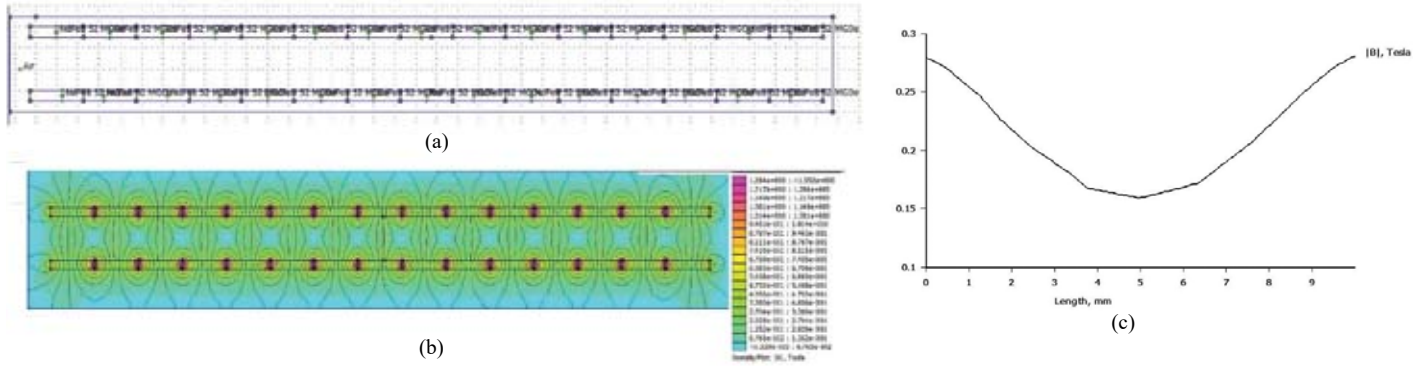


Figure 1. (a) Orientation of permanent magnets, (b) Plot of the magnetic flux density, and (c) Variation of field intensity v/s distance.

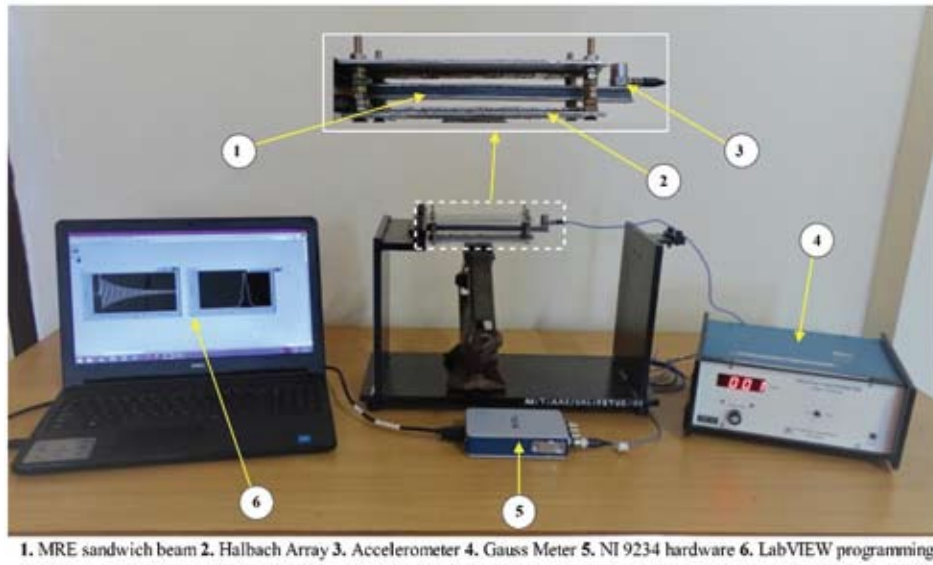


Figure 2. Experimental setup for determining free vibration response.

card and NI LabVIEW. The natural frequency of the specimen is obtained by computing FFT of the acquired signals. The first dominant mode is considered for analysis. The test was conducted for all the specimens with magnetic flux densities varying between 0T - 0.15T with a step size of 0.05T. An average value was derived after repeating the experiment for 5 times which was considered for further analysis.

**4. RESULTS AND DISCUSSION**

**4.1 Loss Factor of the Viscoelastic Material ( $\eta_1$ )**

Loss factor indicates material damping properties of the viscoelastic material. The required values of loss factor ( $\eta_s$ ) and natural frequency ( $f_s$ ) of the sandwich specimens is obtained experimentally from the free vibration test. The impact of addition of iron particles and field intensity on the natural frequency of the sandwich specimen ( $f_s$ ) is presented in subsections 4.1.1. From the obtained values, the loss factor of the viscoelastic material ( $\eta_1$ ) is calculated using equation 1 and discussed in the subsection 4.1.2.

**4.1.1 Natural Frequency ( $f_s$ ) of the Sandwich Specimen**

The change in natural frequency ( $f_s$ ) with varied CIP content under no field condition obtained from the free vibration test is shown in Table 2. Results indicate that with

Table 2. Natural frequencies of the Sandwich specimens determined experimentally and FEM simulation at 0T.

Percentage CIP	Natural frequency (Hz)		
	Experiment	FEM	Percentage variation
0	26.37	27.84	5.574
5	26.42	27.95	5.474
10	26.66	28.44	6.259
15	26.94	28.46	5.341
20	27.17	28.99	6.278
25	27.37	29.45	7.063
30	27.58	29.93	7.852

the addition of the CIP to the matrix, the natural frequency of the beams increases marginally.

For a classical spring-mass system, the equation governing the natural frequency ( $\omega_n$ ) with respect to stiffness ( $k$ ) and mass ( $m$ ) is given as

$$\omega_n = \sqrt{\frac{k}{m}} \tag{7}$$

From equation the impact of iron powder in stiffness enhancement is more than the mass addition in the sample.

The above trends were ascertained by performing modal analysis (3D Finite element method) in Altair Hyperworks suite to determine the natural frequencies of all the specimens at 0T. The finite element model of the sandwich specimen with cantilever boundary condition is shown in Fig. 3(a). The mass loading effect induced by the accelerometer (10grams) is simulated by applying a concentrated mass (CONM2) on the rigid element RBE3 which connects the mesh sets together. 8 nodes hexahedron (Hex 8) was chosen as the type of element for base beam and core material. A node to node connection is established between the aluminium beam and MRE. The material property (Young's modulus) of the core material was specified based on the results obtained by Sandesh<sup>22</sup>, *et al.*. The mode shape of the 1<sup>st</sup> mode of the 0% CIP sample is shown in Fig. 3(b). The natural frequency obtained from finite element method for the all the samples is presented in Table 2 and has been compared with the experimental results. The percentage deviation is less than 8% indicating a good correlation between them.

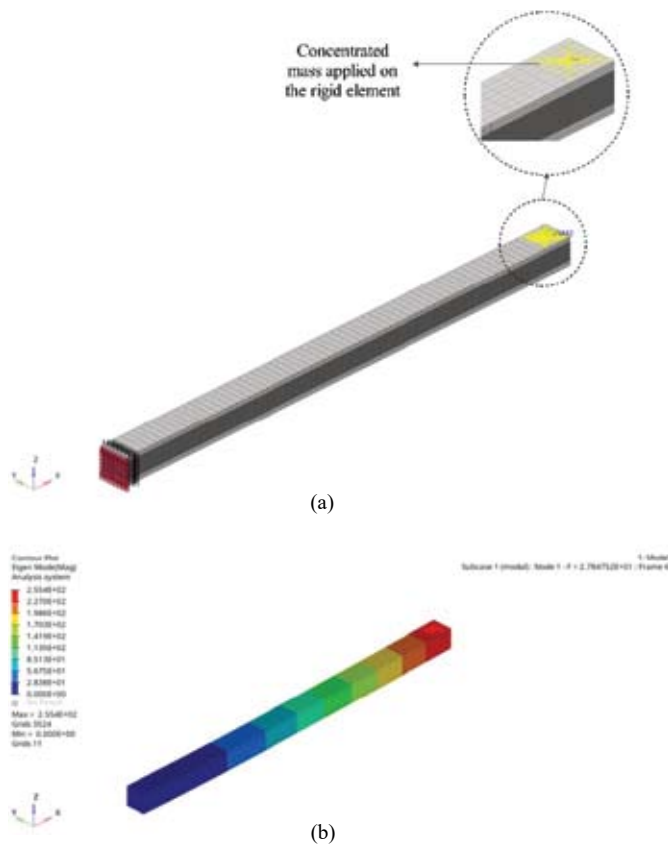


**Figure 3. (a) Finite element model of the sandwich specimen and (b) Mode 1 of the 0% CIP sample.**

The effect of the applied field on the natural frequency of each specimen is depicted in Table 3. The natural frequency decreased with an increase in the magnetic flux density. The natural frequency of 5% MRE sample reduces by 0.75% tested at 0.05T in comparison to 3% reduction of the same sample tested at 0.15T. Also, the natural frequency of 5% MRE sample reduces by 3% in comparison to 14% reduction of 30% MRE sample both tested at 0.15T. These trends of decrease in natural frequency with magnetic field were also described by Kozłowska<sup>23</sup>, *et al.* and Hu<sup>24</sup>, *et al.*.

**Table 3. Variation of natural frequency of the specimens under varied magnetic flux density**

Percentage CIP	Natural frequency (Hz)			
	0T	0.05 T	0.1 T	0.15 T
0	26.37	26.37	26.37	26.37
5	26.42	26.28	26.02	25.62
10	26.66	26.44	25.93	24.61
15	26.94	26.52	25.75	24.90
20	27.17	26.57	25.85	24.72
25	27.37	26.95	26.13	24.51
30	27.58	26.55	25.52	23.72

The decrease in natural frequency of the MRE specimen beam with intensification of the magnetic flux density can be due to the increase in its static deflection<sup>25</sup>. This phenomenon was explained by Rajpal<sup>26</sup>, *et al.*. The fundamental natural frequency ( $\omega_n$ ) of a SDOF system is

$$\omega_n = \sqrt{\frac{g}{\delta}} \quad (8)$$

where  $g$  is the acceleration due to gravity and  $\delta$  is the static deflection of the spring. As per the equation above, an increase in the static deflection of the beam causes its natural frequency to reduce. The static deflection for any MRE sample at no field is zero. With field, the magnetic pull generated by the permanent magnets causes the MRE beam to deflect to a new position increasing its static deflection. Further, the behaviour is pronounced for MRE specimen with higher percentage CIP content leading to a bigger drop in the natural frequency.

#### 4.1.2 Loss Factor ( $\eta_1$ ) of the Viscoelastic Material

The loss factor of the core material is calculated using equation 1. The results obtained are presented in Fig. 4. The loss factor of MRE core material was found to increase with an increase in percentage CIP content and increase in the magnetic flux density.

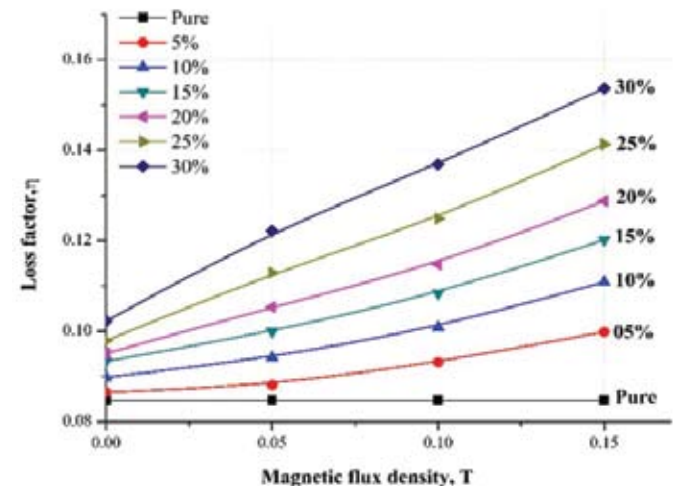


**Figure 4. Loss factor of the viscoelastic material.**

The key aspects contributing to the improvement in the damping characteristics of the core material is explained in this section. The sandwich beam vibrating in flexure, primarily dissipates energy in the form of heat owing to the shear deformation of the viscoelastic layer longitudinally<sup>27</sup>. In addition to this, energy dissipation occurs due to damping effect from the matrix, damping effect from the CIP and energy dissipation between the matrix and the particles due to friction<sup>6,28</sup>. Damping of the pure MRE is due to the inherent damping of the viscoelastic matrix resulting from the friction due to parallel polymer chains (Fig. 5a)<sup>29</sup>. When the CIP particles are embedded, the damping of MRE without the magnetic field can be expressed as<sup>8,29</sup>

$$\eta_{MRE} = \eta_{MAT} + \eta_{CIP} + \eta_{MAT+CIP} \quad (10)$$

where  $\eta_{MRE}$  is the loss factor of the MRE,  $\eta_{CIP}$  is the loss factor of CIP particles and  $\eta_{MAT+CIP}$  is the loss factor due to the friction resulting from the interfacial interaction between the matrix and the CIP particles. The contribution of CIP on damping is minimum and is neglected<sup>30</sup>. Thus, the damping of the MRE majorly depends on the damping provided by the matrix and energy dissipation between the matrix and the CIP particles interface (Fig. 5b). Damping due to interfacial frictional force is a function of number of association points between the CIP particles and the matrix and interactive force between the CIP-Matrix interfaces<sup>8,9</sup>. For samples with higher percentage content of CIP, the number of association points increases causing an increase in interfacial area resulting in energy dissipation due to friction (Fig. 5c)<sup>8,28</sup>. This resulted in the enhancement of the loss factor. Similar trends were observed by Gong<sup>8</sup>.

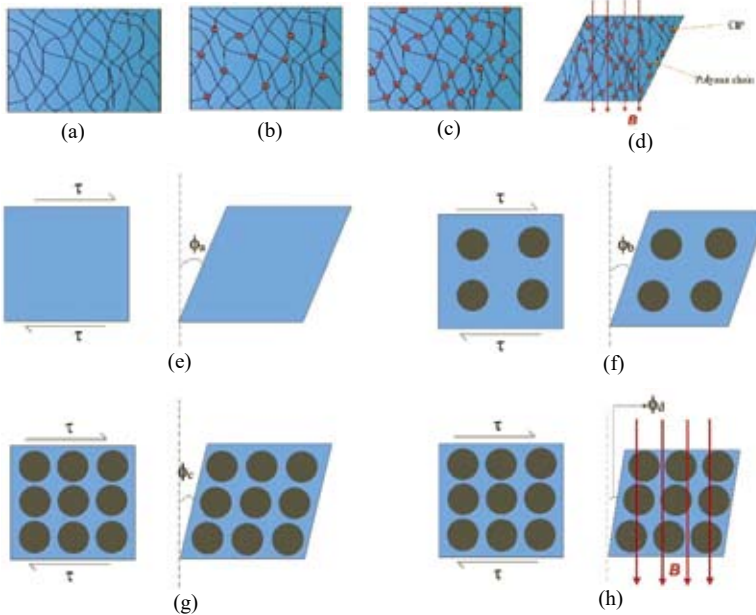


**Figure 5.** (a) Damping due to friction in polymer chains, (b) Damping due to interfacial friction in lower percentage CIP content samples, (c) Damping due to interfacial friction in higher percentage CIP samples, (d) Damping due to applied magnetic field, (e) Variation of Shear strain for pure silicone sample, (f) Variation of Shear strain for 5-20% MRE sample, (g) Variation of Shear strain for 25 and 30% MRE sample, and (h) Variation of Shear strain for MRE sample with applied field.

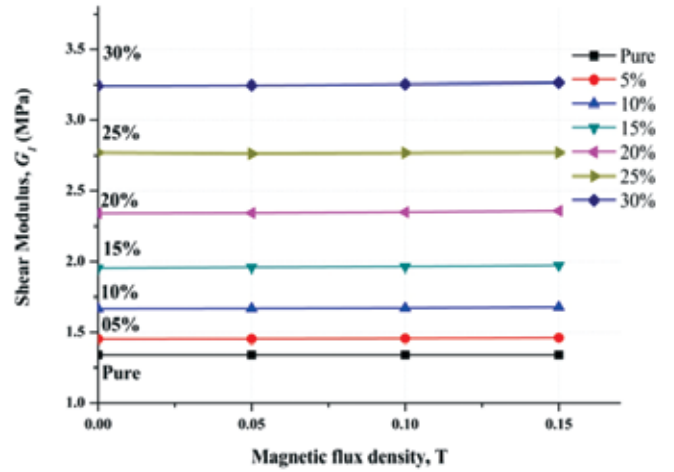


**Figure 6.** Shear modulus of the viscoelastic material.

With the applied field, there is an additional energy dissipation due to the interaction between the adjacent magnetic dipoles<sup>8</sup>.

$$\eta_{MRE} = \eta_{MAT} + \eta_{CIP} + \eta_{MAT+CIP} + \eta_{MF} \quad (11)$$

where  $\eta_{MF}$  is the loss factor resulting from the applied magnetic field. An increase in the magnetic force acting amid the particles and the matrix increases the interactive force between them (Fig. 5d)<sup>8,29</sup>. The increase in the interactive force between them enhances the energy dissipation due to friction.

#### 4.2 Shear Modulus ( $G_j$ ) of the Viscoelastic Material

Shear modulus represents the elastic behaviour (stiffness) of the material. The shear modulus of the core material was calculated using Eqn (2). It was observed that the addition of CIP particles enhances the shear modulus (Fig. 6). These trends obtained agree with the studies conducted by Gong<sup>31</sup> and Yunus<sup>32</sup>.

A unit cell of the MRE matrix was considered to study the variation of shear modulus as a function of percentage content of iron powder and applied field. The pure silicone elastomer has no CIP particles (Fig. 5e). The unit cell is assumed to contain 4 CIP particles (Fig. 5f) for samples with 5-20% CIP content. For samples with 25% and 30% CIP content, the unit cell is assumed to contain 9 CIP particles (Fig. 5g). With the beam vibrating in flexure, the viscoelastic layer experiences shear deformation along the longitudinal direction. The shear strains undergone by the pure silicone, 5-20% MRE and 25-30% MRE samples is denoted as  $\phi_a$ ,  $\phi_b$  and  $\phi_c$  respectively. With the inclusion of the CIP in the pure silicone elastomer, the stiffness of the matrix increases due to the reinforcing effect rendered by the CIP. The shear strain experienced by the 25-30% MRE sample is minimum in comparison to the 5-20% MRE sample and the pure sample. Hence,  $\phi_a > \phi_b > \phi_c$ . The relationship between shear modulus ( $G$ ) and shear stress ( $\tau$ ) and shear strain ( $\phi$ ) is given as

$$G = \frac{\tau}{\phi} \quad (12)$$

Therefore, the Shear modulus of samples with higher percentage content of CIP ( $G_c$ ) is greater in comparison to samples with lesser percentage of CIP ( $G_b$ ). Pure samples have the least shear modulus ( $G_a$ ).

Further, with the applied field, the shear modulus is observed to increase marginally for all the samples. With field, the CIP particles experience a force of attraction causing the distance between them to decrease in the applied field direction due to dipole effect<sup>33</sup>. This arrests the shearing action of the viscoelastic layers in the longitudinal direction causing a decrease in the shear strain  $\phi_d$  as indicated in Fig. 5(h). Hence, the shear modulus increases with field.

## 5. CONCLUSION

In this study, the Viscoelastic properties of RTV silicone based isotropic MRE were characterised by employing ASTM-E756-05. Loss factor and shear modulus variations of the MRE with respect to percentage content of CIP and magnetic field were investigated. The following conclusions are drawn by analysing the results:

- Both Shear modulus and Loss factor were found to increase with an increase in the percentage content of CIP and magnitude of the magnetic flux density.
- Maximum loss factor and Shear modulus were observed for 25% and 30% CIP content samples at 0.1T and 0.15T magnetic field, respectively.
- The stiffness of the samples increased slightly with the addition of the CIP resulting in an improvement in the natural frequency denoting that there is an improvement in stiffness to mass ratio. The behaviour was validated numerically by conducting modal analysis.
- The increase in static deflection due to magnetic pull experienced by the beam due to the applied field resulted in decrease of its natural frequencies of the specimen.

## REFERENCES

1. Carlson, J.D. & Jolly, M.R. MR fluid, foam and elastomer devices. *Mechatronics.*, 2000, **10**(4), 555-69. doi:10.1016/S0957-4158(99)00064-1.
2. Li, W. & Zhang, X. Research and applications of MR elastomers. *Recent Patents on Mechanical Engineering.* 2008, **1**(3),161-66. doi:10.2174/1874477X10801030161.
3. Li, Y.; Li, J.; Li, W. & Du, H. A state-of-the-art review on magnetorheological elastomer devices. *Smart Mater. Struct.*, 2014, **23**(12). doi: 10.1088/0964-1726/23/12/123001.
4. Ginder, J.M.; Nichols, M.E.; Elie, L.D. & Tardiff, J.L. Magnetorheological elastomers: properties and applications. *In Smart Structures and Materials*, CA, United States, 1999. doi: 10.1117/12.352787.
5. Nanthakumar, A.J.; Jancirani, J.; Rajasekaran, S.C. & Sarathkumar, K. Multiphysics Analysis of a Magnetorheological Damper. *Def. Sci. J.*, 2019, **69**(3), 230-35. doi:10.14429/dsj.69.14424.
6. Thakur, M.K. & Sarkar, C. Experimental and Numerical Study of Magnetorheological Clutch with Sealing at Larger Radius Disc. *Def. Sci. J.*, 2020, **70**(6), 575-82 doi:10.14429/dsj.70.15778.
7. Zhang, X.; Li, W. & Gong, XL. An effective permeability model to predict field-dependent modulus of magnetorheological elastomers. *Commun. Nonlinear Sci. Numerical Simulation*, 2008, **13**(9), 1910-16. doi:10.1016/j.cnsns.2007.03.029
8. Chen, L.; Gong, X.L. & Li, W.H. Damping of magnetorheological elastomers. *Chin. J. Chem. Phys.*, 2008, **21**(6), 581-86. doi:10.1088/1674-0068/21/06/581-585
9. Li, J.F. & Gong, XL. Dynamic damping property of magnetorheological elastomer. *J. Cent. South Univ. Technol.*, 2008, **15**(1), 261-65. doi: 10.1007/s11771-008-359-2
10. Hegde, S.; Poojary, U.R. & Gangadharan, K.V. Experimental investigation of effect of ingredient particle size on dynamic damping of RTV Silicone base Magnetorheological elastomers. *International Conference on Advances in Manufacturing and Materials Engineering*, Mangalore, Karnataka, 2014. doi: 10.1016/j.mspro.2014.07.473.
11. Song, H.; Padalka, O.; Wereley, N. & Bell, R. Impact of nanowire versus spherical microparticles in magnetorheological elastomer composites. *In 50th AIAA/ASME/ASCE/AHS/ASC Structures, Structural Dynamics, and Materials Conference*, Palm Springs, California, 2009. doi:10.2514/6.2009-2118.
12. Zhou, GY. Shear properties of a magnetorheological elastomer. *Smart Mater. Struct.*, 2003, **12**(1), 139-46. doi: 10.1088/0964-1726/12/1/316.
13. Kim, YK.; Bae, HI.; Koo, JH.; Kim, KS. & Kim, S. Note: Real time control of a tunable vibration absorber based on magnetorheological elastomer for suppressing tonal vibrations. *Rev. Sci. Instrum.*, 2012, **83**(4). doi: 10.1063/1.4704455
14. Hoang, N.; Zhang, N. & Du, H. A dynamic absorber with a soft magnetorheological elastomer for powertrain vibration suppression. *Smart Mater. Struct.*, 2009, **18**(7), 1-10. doi:10.1088/0964-1726/18/7/074009
15. Li, W.; Zhang, X. & Du, H. Development and simulation evaluation of a magnetorheological elastomer isolator for seat vibration control. *J. Intell. Mater. Syst. Struct.*, 2012 **23**(9), 1041-48. doi: 10.1177/1045389X11435431
16. Liao, G.J.; Gong, X.L.; Xuan, S.H.; Kang, C.J. & Zong, L.H. Development of a real-time tunable stiffness and damping vibration isolator based on magnetorheological elastomer. *J. Intell. Mater. Syst. Struct.*, 2012, **23**(1), 25-33. doi: 10.1177/1045389X11429853
17. Nayak, B.; Dwivedy, SK. & Murthy, KS. Fabrication and characterization of magnetorheological elastomer with carbon black. *J. Intell. Mater. Syst. Struct.*, 2015, **26**(7), 830-39. doi: 10.1177/1045389X14535011

18. Li, WH.; Zhou, Y. & Tian, TF. Viscoelastic properties of MR elastomers under harmonic loading. *Rheol Acta.*, 2010, **49**(7), 733-40.  
doi:10.1007/s00397-010-0446-9.
19. ASTM standard. Standard test method for measuring vibration damping properties of materials. E 756-05: 2011, United States. ASTM, 2011.
20. Pope, D. Halbach Arrays Enter the Maglev Race, The Industrial physicist. <https://www.yumpu.com/en/document/read/23120490/halbach-arrays-enter-the-maglev-race>
21. Gorman, D.; Jerrams, S.; Ekins, R. & Murphy, N. Creating a uniform magnetic field for the equi-biaxial physical testing of magnetorheological elastomers; Electromagnet design, development and testing. ECCMR VII- The 7<sup>th</sup> European Conference on Constitutive models for Rubber, DIT, Dublin, 2011.  
doi:1201/b11687-75.
22. Sandesh, B.; Sriharsha, H.; Sathish, UR. & Nikhil, G. Investigation of tensile properties of RTV Silicone based Isotropic Magnetorheological Elastomers. In MATEC Web of Conferences, Manipal, Karnataka, 2018.  
doi: 10.1051/mateconf/201714402015.
23. Kozłowska, J.; Boczkowska, A.; Czulak, A.; Przybyszewski, B.; Holeczek, K.; Stanik, R. & Gude, M. Novel MRE/CFRP sandwich structures for adaptive vibration control. *Smart Mater. Struct.*, 2016, **25**(3), 1-11.  
doi:10.1088/0964-1726/25/3/035025.
24. Hu, G.; Guo, M.; Li, W.; Du, H. & Alici, G. Experimental investigation of the vibration characteristics of a magnetorheological elastomer sandwich beam under non-homogeneous small magnetic fields. *Smart Mater. Struct.*, 2011, **20**(12), 1-7.  
doi:10.1088/0964-1726/20/12/127001
25. Rajpal, R.; Lijesh, KP.; Kant, M. & Gangadharan, KV. Experimental study on the dynamic properties of magnetorheological materials. In IOP Conference Series: Materials Science and Engineering, Kattankulathur, 2018.  
doi:10.1088/1757-899X/402/1/012140
26. Rajpal, R.; Lijesh, KP. & Gangadharan KV. Experimental investigation of 3D-printed polymer-based MR sandwich beam under discretized magnetic field. *J. Braz. Soc. Mech. Sci. Eng.*, 2018, **40**(12), 1-11.  
doi:10.1007/s40430-018-1488-7
27. Hao, M. & Rao, MD. Vibration and damping analysis of a sandwich beam containing a viscoelastic constraining layer. *J. Compos. Mater.*, 2005, **39**(18),1621-43.  
doi: 10.1177/0021998305051124
28. Yang, J.; Gong, X.; Deng, H.; Qin, L. & Xuan, S. Investigation on the mechanism of damping behavior of magnetorheological elastomers. *Smart Mater Struct.*, 2012, **21**(12), 1-11.  
doi:10.1088/0964-1726/21/12/125015
29. Fay, JJ.; Murphy, CJ.; Thomas, DA. & Sperling, LH. Effect of morphology, crosslink density, and miscibility on interpenetrating polymer network damping effectiveness. *Polymer Eng. Sci.* 1991, **31**(24), 1731-41.  
doi:10.1088/0964-1726/20/3/035007.
30. Ju, BX.; Yu, M.; Fu, J.; Yang, Q.; Liu, XQ. & Zheng, X. A novel porous magnetorheological elastomer: preparation and evaluation. *Smart Mater Struct.*, 2012, **21**(3),1-10.  
doi:10.1088/0964-1726/21/3/035001
31. Gong, XL.; Chen, L. & Li, JF. Study of utilizable magnetorheological elastomers. *Int. J. Mod. Phys. B.*, 2007, **21**(28n29), 4875-82.  
doi: 10.1142/S0217979207045785.
32. Yunus, NA.; Mazlan, SA.; Choi, SB.; Imaduddin, F. Aziz, SA. & Khairi, MH. Rheological properties of isotropic magnetorheological elastomers featuring an epoxidized natural rubber. *Smart Mater. Struct.*, 2016, **25**(10),1-11.  
doi:10.1088/0964-1726/25/10/107001
33. Poojary, UR.; Hegde, S. & Gangadharan, KV. Dynamic blocked transfer stiffness method of characterizing the magnetic field and frequency dependent dynamic viscoelastic properties of MRE. *Korea Aust. Rheol. J.*, **28**(4), 301-13.  
doi: 10.1007/s13367-016-0031-6

#### ACKNOWLEDGEMENT

The experimental facility was provided by Vibrations and Acoustics laboratory, at Department of Aeronautical and Automobile Engineering at MIT, Manipal.

#### CONTRIBUTORS

**Mr Sandesh Bhaktha** obtained his Mtech degree from Manipal Institute of Technology, Manipal in 2017 and currently pursuing his PhD from NITK, Surathkal. He has worked as an Assistant Professor in the Department of Mechanical Engineering at Shri Madhwa Vadiraja Institute of Technology and Management, Udupi (2017-2018). His research areas include Automotive NVH, Smart materials, Finite element solutions and Electrical mobility.

His contribution in the present study includes fabrication of test specimens, conducting experiments, FEM simulations and analysis of results and discussions.

**Dr Sriharsha Hegde** obtained his PhD from NITK, Surathkal and MTech from NIT, Calicut. He is working as Assistant Professor-senior scale in Aeronautical and Automobile Engineering Department at Manipal Institute of Technology since 2015. His area of interests includes Smart Materials, Vibrations, and Instrumentation.

His contribution in the present study includes the overall supervision, conducting analysis of the results and preparing the manuscript.

**Dr Sathish Rao U.** obtained his PhD from Manipal University, Manipal in Composite Machining Optimisation. He is working as Associate Professor - Senior Scale in the Department of Mechanical and Manufacturing Engineering at Manipal Institute of Technology, Manipal since 2009. His area of interests includes Composite Material Fabrication and characterisation, Design of Experiments, Manufacturing and Machining optimisation.

His contribution in the present study includes the project guidance, discussion regarding the results obtained, preparation of project report and technical paper.